Time-dependent photon migration using path integrals

Lev T. Perelman, Jun Wu, Yang Wang, Irving Itzkan, Ramachandra R. Dasari, and Michael S. Feld
George R. Harrison Spectroscopy Laboratory, Massachusetts Institute of Technology, Cambridge, Massachusetts 02139
(Received 6 January 1995)

We present an approach to the problem of light propagation in turbid media based on the path integral formalism. The method of analysis provides solutions to the time-dependent equation of radiative transfer for a number of cases for which known approximations, including the diffusion approximation, are not applicable. The theory and experiments show that trajectories of photon traversing a turbid medium cluster around a well defined, time-resolved path called a classical path. This concept is a powerful tool, and it provides physical insight into optical propagation in turbid media.

PACS number(s): 42.68.Ay, 87.59.Wc, 05.60.+w, 78.20.Dj

I. INTRODUCTION

The study of light propagation in a highly scattering or turbid medium is of great current interest, especially because of recent potential applications to medical problems, such as imaging. (For a review of recent work see [1]). Unfortunately, in most realistic situations, the analytical solution to the equation of radiative transfer is not known, and the limiting cases in which approximate solutions can be obtained (diffusion approximation, the Kubelka-Munk approximation, etc.) are not always relevant for applications such as medical imaging. This paper presents an approach in which the integral-differential radiative transfer equation is reformulated in terms of a path integral [2,3]. The approach provides new solutions to the problem of light propagation in turbid media, as well as new insights into the physical basis of the process.

The most important issue to be addressed in performing optical imaging in a turbid medium is the type of photons to be used: (i) nonscattering, (ii) scattered along almost straight line (low-diffusive) or (iii) highly diffusive. Obviously, (i) provides the most precise information. In this case the problem can be analyzed by using geometrical optics. Unfortunately simple estimates show that it is nearly impossible to detect such photons for realistic geometries: the number of nonscattered photons decreases as $\sim\exp-(\mu_a+\mu_S)L$, with L is the distance between the source and detector. For realistic biological tissue, μ_S is of the order of 100 cm^{-1}, which makes signals almost undetectable for $L>1$ cm. The other limit (iii) does not suffer from this problem—a large number of highly randomized photons can reach the detector but, unfortunately, because of the randomization which accompanies multiple scattering, it is very difficult to extract imaging information from the detected photons. Thus it is important to explore the intermediate regime of case (ii). Its main problem is the absence of accurate analytic solutions in the limit where the diffusion approximation does not hold.

As shown below, the path integral formalism can provide solutions which exhibit causality and contain information about low-randomized photons. The other advantage of the path integral approach is its introduction of the concept of the classical path, which describes the region of space where the largest number of the photon trajectories are clustered. Knowledge about the position of the classical path can be used to extract optical information in turbid media.

Photons propagating through a turbid medium from point **A** to point **B** can be described using statistical considerations. A photon originating at point **A** is elastically scattered multiple times, each time being deflected into a particular angle with a well-defined probability, thus forming a trajectory within the medium. Each trajectory has a particular probability. By calculating this probability and then summing over all possible trajectories, one obtains the probability for the photon to travel between two points in the medium. Monte Carlo modeling, the standard numerical method for solving the radiative transfer equation, simulates this process but does not estimate the probability for a full trajectory.

The probability for a photon to traverse the scattering medium from point **A** with radius vector $\mathbf{r}_A$ to point **B** with radius-vector $\mathbf{r}_B$ in a time interval T can be written as a path integral [4]:

$$P(\mathbf{r}_A,\mathbf{r}_B,T)=\int \mathcal{D}\mathbf{r}(t)\exp\left[-\frac{1}{2\mu_S(1-g)}\int_0^T[\dot{\mathbf{r}}(t)]^2dt\right]\times J(\dot{\mathbf{r}}(t))\,, \tag{1}$$

where the function

$$J(\dot{\mathbf{r}}(t))=\int \mathcal{D}\Omega(t)\exp\left\{i\mu_S\int_0^T dt\,\Omega(t)([\dot{\mathbf{r}}(t)]^2-1)\right\}$$

ensures that photons propagate at the speed of light in the medium ($c=1$) at every point along the trajectory, and $\mathcal{D}\mathbf{r}(t)=\prod_{n=1}^{N}d\mathbf{r}_n$. Here, integrals over all possible intermediate points of the trajectory have to be calculated using appropriate limits: from $-\infty$ to $+\infty$ for an infinite medium, from $-\infty$ to 0 for semi-infinite geometries, and so on. In this paper we shall always consider the infinite geometry case, unless otherwise specified. Integral (1) represents the solution of the equation of radiative transfer for the case in which elastic

scattering is described by a Gaussian phase function. Although Eq. (1) can be derived in a rigorous manner [2,3], here we instead present a simplified but physically intuitive approach in which photons travel exactly one scattering length l_S between two consecutive scattering events.

II. PRELIMINARY CONSIDERATIONS

Consider a photon traversing a turbid medium at the speed of light, $c=1$, which undergoes elastic scattering each time it travels exactly one scattering length l_S, where the inverse scattering length or scattering coefficient $\mu_S=l_S^{-1}$. The probability that a scattering event at point i deflects the photon into the solid angle $d\Theta_i=\sin\vartheta_i d\vartheta_i d\varphi_i$ can be written in the form $p(\vartheta_i)\sin\vartheta_i d\vartheta_i d\varphi_i$ with $p(\vartheta_i)$ the phase function [5]. In a turbid medium, $p(\vartheta_i)$ is well described by a Gaussian function

$$p(\vartheta_i)=\frac{1}{\pi\langle\vartheta^2\rangle}\exp\left[-\frac{\vartheta_i^2}{\langle\vartheta^2\rangle}\right], \tag{2}$$

with $\langle\vartheta^2\rangle$ the averaged square of the scattering angle. In terms of the anisotropy parameter $g=\langle\cos\vartheta\rangle$, $g\cong 1-\frac{1}{2}\langle\vartheta^2\rangle$ for small angles. The constant in front of the exponential term ensures that the total probability for a photon to be scattered in all possible angles equals unity. The probability distribution for the photon after the scattering event is then

$$P(\mathbf{r}_i,\mathbf{r}_{i-1})d^3\mathbf{r}_i=\frac{1}{\mu_s\pi(1-g)}\exp\left[-\frac{\vartheta_i^2}{2(1-g)}\right]\times\sin\vartheta_i d\vartheta_i d\varphi_i d\xi_i\delta(\xi_i^2-\mu_S^{-2}), \tag{3}$$

where $d^3\mathbf{r}_i=dx_i dy_i dz_i$, and $\boldsymbol{\xi}_i=\mathbf{r}_i-\mathbf{r}_{i-1}$. Here, each scattering event is labeled with an index i, so that $i=0$ is the starting point, **A**, and $i=N+1$ is the finishing point, **B**. The number of scattering events, N, is related to the travel time, T, by $N=\mu_S T$.

Equation (3) can be rewritten in terms of the coordinates $\mathbf{r}_i$. Making the small angle approximation $\vartheta_i=\mu_S\sqrt{(\mathbf{r}_{i+1}+\mathbf{r}_{i-1}-2\mathbf{r}_i)^2}$ (which simplifies the calculation but is not essential), we obtain

$$P(\mathbf{r}_{i+1},\mathbf{r}_i)=\frac{1}{\mu_S\pi(1-g)}\exp\left[-\frac{\mu_S^2}{2(1-g)}(\mathbf{r}_{i+1}+\mathbf{r}_{i-1}-2\mathbf{r}_i)^2\right]\times\delta((\mathbf{r}_{i+1}-\mathbf{r}_i)^2-\mu_S^{-2}). \tag{4}$$

The probability for the photon to traverse the scattering medium along a particular trajectory is given by the product of probabilities, Eq. (4), at each point along the trajectory. Writing $\dot{\mathbf{r}}_i=\mu_S(\mathbf{r}_{i+1}-\mathbf{r}_i)$, and $\ddot{\mathbf{r}}_i=\mu_S^2(\mathbf{r}_{i+1}+\mathbf{r}_{i-1}-2\mathbf{r}_i)$, with each raised dot signifying a time derivative, we can now express this probability as an integral over all possible paths:

$$P(\mathbf{r}_A,\mathbf{r}_B,T)=\int\int\cdots\int d\mathbf{r}_1 d\mathbf{r}_2\cdots d\mathbf{r}_N[\mu_S\pi(1-g)]^{-N}\exp\left[-\frac{1}{2\mu_S(1-g)}\int_0^T[\ddot{\mathbf{r}}(t)]^2dt\right]\prod_{i=1}^{N}\delta(\dot{\mathbf{r}}_i^2-1). \tag{5}$$

The exponential term in Eq. (5) plays the role of the action term $\exp(-iS/\hbar)$ in Feynman's formulation of quantum mechanics [6] and, following this notation, we call $S_{\text{eff}}=\int_0^T[\ddot{\mathbf{r}}(t)]^2dt$ the effective classical action for a photon in a turbid medium. The function $J(\dot{\mathbf{r}}(t))=\prod_{i=1}^{N}\delta(\dot{\mathbf{r}}_i^2-1)$ represents the density of trajectories along which the photon speed equals unity. As shown in Appendix A, this function can be written as a path integral [Eq. (A2)]. Combining all terms, we immediately obtain Eq. (1).

III. DIFFUSIVE LIMIT

The probability distribution function for the case of isotropic scattering, generally referred to as the diffusive limit [5], does not follow immediately from Eq. (1), which was derived in the approximation of small angle scattering. However, the approach presented in Sec. II can be directly applied to the case of diffusive scattering by simply eliminating the angular dependence of the phase function. Thus in this case $P(\mathbf{r}_A,\mathbf{r}_B,T)$ is a path integral over the function $J(\dot{\mathbf{r}}(t))$,

$$P(\mathbf{r}_A,\mathbf{r}_B,T)=\int_A^B\mathcal{D}\mathbf{r}(t)J(\dot{\mathbf{r}}(t)). \tag{6}$$

The calculation can be further simplified by rewriting the path integral in the form of a Fourier transform. The approximation of Eq. (A3) then gives:

$$J(\dot{\mathbf{r}}(t))=Q\int_{-\infty}^{+\infty}d\omega\exp\left[-i\omega\int_0^T dt([\dot{\mathbf{r}}(t)]^2-1)\right]. \tag{7}$$

Physically, this means that we constrain the average speed of the photon over its trajectory to unity, rather than its instantaneous velocity. Interestingly enough, this approximation does not change the final result for the isotropic case, which can be derived rigorously.

We then compute the integral as

$$P(\mathbf{r}_A,\mathbf{r}_B,T)=\int_A^B\mathcal{D}\mathbf{r}(t)\times\int_{-\infty}^{+\infty}d\omega Q\times\exp\left[-i\omega\int_0^T dt([\dot{\mathbf{r}}(t)]^2-1)\right]. \tag{8}$$

Since in this case the scattering is isotropic, each scattering can reorient the photon by an arbitrary angle with equal probability, so the orientations of the initial and final velocities are obviously not important. The trajectory can be written as a Fourier sine series with a fundamental period of T [6]. Thus

$$\mathbf{r}(t)=\frac{\mathbf{R}}{T}t+\sum_{n=1}^{N/2}\left\{\mathbf{a}_n \sin\left[\frac{\pi nt}{T}\right]+\mathbf{b}_n \cos\left[\frac{\pi nt}{T}\right]\right\}, \quad (9)$$

where the number of constants $\mathbf{a}_n$ and $\mathbf{b}_n$ is equal to the number of intermediate coordinates that prescribed the trajectory, which is $3N$. The initial and final conditions for the trajectory can be chosen to be of the form $\mathbf{r}(0)=\mathbf{0}$, $\mathbf{r}(T)=\mathbf{R}$ which leaves only sin terms in Eq. (9). As discussed in Ref. [6], the trajectories may be considered to be functions of the coefficients $\mathbf{a}_n$ instead of $\mathbf{r}$. This is a linear transformation whose Jacobian is only a function of T. Then $\mathcal{D}\mathbf{r}(t)\propto\prod_{n=1}^{N/2}d\mathbf{a}_n$, and Eq. (8) reduces to

$$P(\mathbf{r}_A,\mathbf{r}_B,T)=F(T)\int_{-\infty}^{+\infty}d\omega\prod_{n=1}^{N/2}\int_{-\infty}^{+\infty}d\mathbf{a}_n \exp\left\{-i\omega T\left[\frac{\mathbf{R}^2}{T^2}-1+\frac{1}{2}\left[\frac{\pi n}{T}\right]^2\mathbf{a}_n^2\right]\right\}, \quad (10)$$

where the function $F(T)$ can be determined from normalization of the probability. Each of integrals of $\mathbf{a}_n$ can be completely separated and calculated independently, so we have

$$P(\mathbf{r}_A,\mathbf{r}_B,T)=F(T)\int_{-\infty}^{+\infty}d\omega \exp\left[i\omega T\left[1-\frac{\mathbf{R}^2}{T^2}\right]\prod_{n=1}^{N/2}\left[\frac{2iT}{\pi n^2\omega}\right]^{3/2}\right], \quad (11)$$

This last integral can be calculated in the standard way by adding a small imaginary part to ω and then allowing it to tend to zero: $\omega\Longrightarrow\omega+i\varepsilon$ with $\varepsilon\rightarrow 0$. This gives

$$P(\mathbf{R},T)=\lim_{\varepsilon=0}F(T)\left[\frac{2iT}{\pi}\right]^{3N/4}\prod_{n=1}^{N/2}n^{-3}\int_{-\infty}^{+\infty}d\omega(\omega+i\varepsilon)^{-3N/4}\exp\left[i\omega T\left[1-\frac{\mathbf{R}^2}{T^2}\right]\right]. \quad (12)$$

This integral takes on different values for $R>T$ and $R<T$ [7]. In the first case it is equal to zero, which simply reflects the requirement of causality—there is not enough time for photon initially at **A** to get to point **B**. In the second case it is proportional to $(1-\mathbf{R}^2/T^2)^{3N/4}$, and we can combine all spatially independent terms inside $F(T)$. This gives

$$P(\mathbf{R},T)=\begin{cases}0\ , & R>T\\ F(T)\left[1-\dfrac{\mathbf{R}^2}{T^2}\right]^{3\mu_S T/4}, & R<T\end{cases} \quad (13)$$

where we utilize the fact that $N=\mu_S T$. The function $F(T)$ can be found from the normalization condition

$$\int_0^T F(T)\left[1-\frac{R^2}{T^2}\right]^{3\mu_S T/4}R^2dR=1\ , \quad (14)$$

which means that photon has to be found somewhere in space, so that the overall probability equals unity. This gives

$$F(T)=\frac{2}{T^3B(3/2,3\mu_S T/4+1)}\ ,$$

where $B(\alpha,\beta)$ is the β function [7],

$$P(\mathbf{R},t)=\frac{2}{T^3B(3/2,3\mu_S T/4+1)}\times\exp\left\{\frac{3\mu_S T}{4}\ln\left[1-\frac{\mathbf{R}^2}{T^2}\right]\right\}, \quad (15)$$

When $R\ll T$, we immediately obtain

$$P(\mathbf{R},T)\cong\left[\frac{3\mu_S}{4\pi T}\right]^{3/2}\exp\left\{-\frac{3\mu_S\mathbf{R}^2}{4T}\right\}. \quad (16)$$

This formula is a standard result of the time dependent diffusion approximation. As easy to see, Eq. (13) has the correct properties for short times $R\sim T$. In contrast, causality is not preserved in the standard diffusion approximation.

IV. SMALL ANGLE SCATTERING REGIME

We next consider the much more important and interesting case for which scattering is not isotropic and the phase function is highly peaked in the forward direction. This is the case of relevance to biological tissue. The solution to the transport equation for a sample of infinite extent is given by the integral Eq. (1), which we simplify in our standard way by choosing the density of trajectories, $J(\dot{\mathbf{r}}(t))$, in the form of Eq. (A3). We then obtain

$$P(\mathbf{r}_A,\mathbf{r}_B,T)=\int_{-\infty}^{+\infty}d\omega\int\mathcal{D}\mathbf{r}(t)Q\exp\left[-\int_0^T\left[\frac{1}{2\mu_S(1-g)}[\ddot{\mathbf{r}}(t)]^2-i\omega([\dot{\mathbf{r}}(t)]^2-1)\right]dt\right]. \quad (17)$$

The same approach employed in the previous section can be used to evaluate this integral. We represent the trajectory $\mathbf{r}(t)$ as the sum of two terms. The first term, which we call the classical path, $\mathbf{r}_{\rm cl}(t)$, is the function in the exponent that minimizes the real part and satisfies the initial and final conditions for coordinates and velocities (see [2] and Appendix

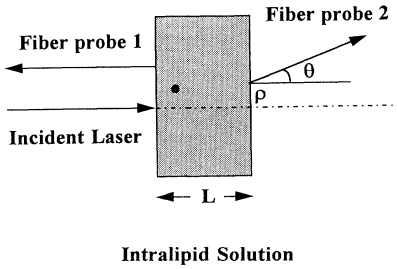

FIG. 1. Schematic diagram of experimental geometry. Experiment 1 uses fiber probe 1 with an absorbing object present ($L=18$ cm). Experiment 2 uses fiber probe 2 without an absorbing object in the intralipid solution ($L=5.5$ cm).

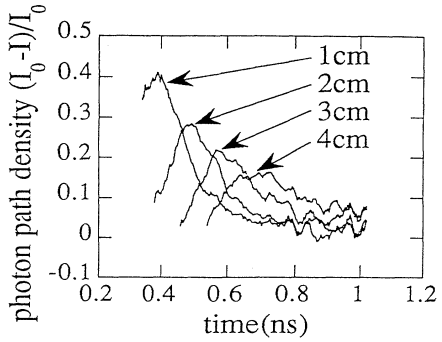

FIG. 2. Normalized photon path distribution measured by placing the absorbing structure along the midline between the incident light and collection fiber.

B). The second term, $\mathbf{q}(t)$, describes the variation around this classical path that allows us to satisfy the constraint on photon speed. We thus have

$$\mathbf{r}(t)=\mathbf{r}_{\rm cl}(t)+\mathbf{q}(t)\ . \tag{18}$$

Using this representation for $\mathbf{r}(t)$, we can write the probability $P(\mathbf{r}_A,\mathbf{r}_B,T)$ in the following form:

$$P(\mathbf{r}_A,\mathbf{r}_B,T)=Q\exp\left[-\int_0^T\left[\frac{1}{2\mu_S(1-g)}\ddot{\mathbf{r}}_{\rm cl}^2\right]\right]\int_{-\infty}^{+\infty}d\omega\exp\left[i\omega\int_0^T(\dot{\mathbf{r}}_{\rm cl}^2-1)dt\right]$$
$$\times\int\mathcal{D}\mathbf{q}\exp\left[-\int_0^T\left[\frac{1}{2\mu_S(1-g)}\ddot{\mathbf{q}}^2-i\omega(2\dot{\mathbf{r}}_{\rm cl}\dot{\mathbf{q}}+\dot{\mathbf{q}}^2)\right]dt\right], \tag{19}$$

where the function $\mathbf{q}(t)$ is chosen to satisfy the boundary conditions $\mathbf{q}(0)=\dot{\mathbf{q}}(0)=\mathbf{q}(T)=\dot{\mathbf{q}}(T)=0$. This integral is approximately equal to (Appendix C)

$$P(\mathbf{r}_A,\mathbf{r}_B,T)=F(T)\exp\left[-\int_0^T\frac{1}{2\mu_S(1-g)}\ddot{\mathbf{r}}_{\rm cl}^2dt-\frac{3\mu_S(1-g)T^2}{2}\left[\int_0^T(1-\dot{\mathbf{r}}_{\rm cl}^2)dt\right]^{-1}\right], \tag{20}$$

where, as before, $F(T)$ is a normalization function. If we consider a slab of thickness L and introduce a coordinate system so that the x and y axes are parallel to the slab's surface and z is normal to this surface, then we can approximately write

$$P(\mathbf{r}_A,\mathbf{r}_B,\mathbf{W},T)=Q\left[\frac{3\mu_S(1-g)}{4\pi}\right]^{3/2}T^{-5/2}\left[1-\frac{(L^2+\mathbf{D}^2)}{T^2}\right]^{3\mu_S(1-g)T/4}$$
$$\times\exp\left\{-\frac{12}{\mu_S(1-g)T^3}\left[L^2+\left[\mathbf{D}-\frac{\mathbf{W}T}{2}\right]^2\right]-\frac{\mathbf{W}^2}{\mu_S(1-g)T}\right\}, \tag{21}$$

where $\mathbf{D}=(D_x,D_y)$ is a vector that represents displacement of the detected photon from the slab's axes and the vector $\mathbf{W}$ describes the angle at which the photon emerges from the slab. The components of $\mathbf{W}=(W_x,W_y)$ are the angles it makes with the x-z and y-z planes, respectively, and Q is a normalization constant.

As can be seen, the probability depends upon the two factors, one resembling the "diffusion" term [Eq. (13)], which dominates in the long time limit, and the second, which comes into play at short times, and is most important for the early photons that follow short, "almost straight" trajectories.

V. EXPERIMENT AND COMPARISON WITH THEORY

Two sets of experiments were carried out to study qualitatively and quantitatively features of photon paths

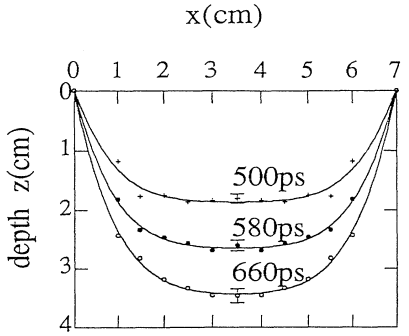

FIG. 3. Experimentally measured photon paths for backscattering geometry.

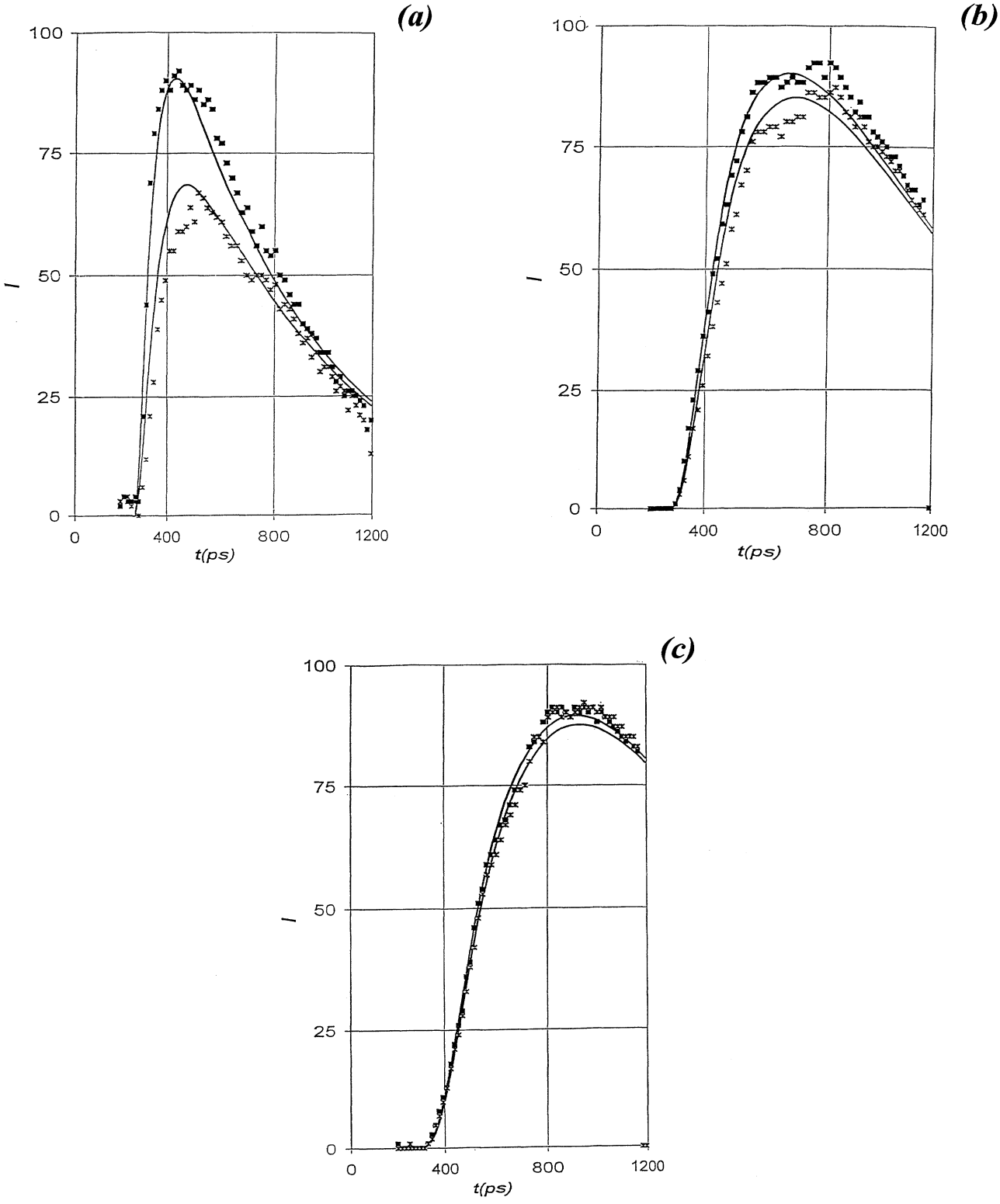

FIG. 4. Time-resolved signal I for transmission (a.u.) through the slab of turbid media with thickness $L=5.5$ cm. Different curves represent two different angles of the problem $\theta=40°$ and $\theta=-40°$ displaced on $D_x=2$ cm from the axes of symmetry. Experiment (dots) (a) $C_{\text{intr}}=10$ ml, (b) $C_{\text{intr}}=15$ ml, and (c) $C_{\text{intr}}=20$ ml vs theory (solid lines) (a) $\mu_S=3\ \text{cm}^{-1}$, $g=0.8$, (b) $\mu_S=6\ \text{cm}^{-1}$, $g=0.8$, and (c) $\mu_S=8\ \text{cm}^{-1}$, $g=0.8$.

in turbid media (Fig. 1). The experiment used ~150 fs excitation pulses generated by a Coherent Mira 900 mode-locked Ti:sapphire laser pumped by a Coherent Innova 400 multiline argon ion laser, and a streak camera detection system consisting of a Hamamatsu temporal disperser C1587, synchroscan streak unit M1955, and tuning unit M1954. The incident wavelength was 800 nm, the repetition rate 76 MHz, and the average power 1.5 W. A small portion of the excitation light, deflected by a quartz plate to a fast photodiode (D), was used as the optical triggering signal. Transmission signals were collected by a 200 μm core diameter optical fiber. The other end of the fiber was imaged onto the streak camera slit. The system resolution, 10 ps, was determined by the intrinsic response of the streak camera, the temporal dispersion through the optical fibers, and optical trigger jitter.

The first set of experiments was designed to show qualitatively the presence of classical paths, $\mathbf{r}_{\rm cl}(t)$, for a backscattering geometry. A small absorbing sphere (8 mm in diameter) was positioned inside a glass fish tank ($8\times12\times16$) in.^{3} containing dilute intralipid. The separation between the incident laser beam and collection fiber is 7 cm. The scattering length, l_S, is varied between 2 and 10 mm by changing the concentration. The anisotropy coefficient $g=0.75$, which is much smaller than ideal because smaller values of g tend to randomize the photon paths and thus reduce spatial resolution. The absorbing structure was used to probe the photon paths within the scattering medium. To do this, the absorber was placed at a given position within the medium and the time-resolved diffuse reflectance signal was obtained with and without the absorber present, from which the normalized differential signal was obtained (Fig. 2). As can be seen, the resulting curves are very sensitive to the position of the absorbing structure. By varying the position of the absorber in the medium, the time resolved photon path distributions can be mapped out (Fig. 3). Similar experiment can be done for transmission mode (data not shown).

The second set of experiments was designed to check the theoretical predictions, Eq. (21), for the time dependent transmission through the slab of scattering media. The transmission experiments were conducted in a 15 cm diameter cylindrical glass container. For the scattering medium, we used a stock solution consisting 10% intralipid solution diluted in water to the appropriate concentration. The scattering properties of the media were estimated using Ref. [8]. The thickness of the scattering media was 5.5 cm.

We compare experimental data with the theoretical predictions that follow from Eq. (21). Note that the probability calculated in Eq. (21) is the relative intensity $I_{\rm out}/I_{\rm in}$ observed in the transmission experiment. As shown in Fig. 4, good agreement between theory and experiment can be obtained by varying only one parameter, the reduced scattering coefficient $\mu_S'=\mu_S(1-g)$. This agreement exists not only for the decreasing ("diffusive") part of the curve, but also for the increasing part which represents the earliest highly "nondiffusive" photons. Moreover, Fig. 4 suggests that Eq. (21) has the correct angular dependence. The scattering coefficients and anisotropy factor that we used here, $\mu_S=3.0$, 6.0, 8.0 cm^{-1}, and $g=0.8$ are not exactly the same as suggested by Ref. [8] ($\mu_S=4.0$, 6.0, 8.0 cm^{-1}, and $g=0.7$), but close enough to be in the range of experimental error. The disagreement is larger for small values of μ_S, which corresponds to the lowest intralipid concentration. Rough estimates indicate that this difference can be explained by the effects of the collimated beam.

VI. CONCLUSION

As can be seen, the path integral approach can be quite valuable for the problem of light propagation in turbid media. Although this technique is more complicated than the standard diffusion approximation, it overcomes the main problem of that approximation, namely: how to consider the nonrandomized or earliest photons, which can provide valuable imaging information in highly scattering media.

ACKNOWLEDGMENTS

We gratefully acknowledge loan of the streak camera from Hamamatsu Photonics Systems, Bridgewater, NJ. This research was conducted under support of NIH Grant No. P41-RP02594 and NSF Grant No. CHE 9304251.

APPENDIX A: DENSITY FUNCTION

The density of trajectories, $J(\dot{\mathbf{r}}(t))$, can itself be written as a path integral, using the Fourier transform of the δ function,

$$J(\dot{\mathbf{r}}(t))=\left[\frac{1}{2\pi}\right]^N\prod_{i=1}^{N}\int_{-\infty}^{+\infty}\exp\{i\Omega_i(\dot{\mathbf{r}}_i^2-1)\}d\Omega_i$$
$$=\left[\frac{1}{2\pi}\right]^N\int\int\cdots\int d\Omega_1 d\Omega_2\cdots d\Omega_N\exp\left[i\sum_{k=1}^{N}\Omega_i(\dot{\mathbf{r}}_i^2-1)\right]. \tag{A1}$$

The last expression can be easily rewritten in the form of a path integral:

$$J(\dot{\mathbf{r}}(t))=\left[\frac{1}{2\pi}\right]^N\int_0^0\mathcal{D}\Omega(t)\exp\left[i\mu_S\int_0^T\Omega(t)(\dot{\mathbf{r}}_i^2-1)dt\right]. \tag{A2}$$

The limits of integration here mean that initial and final points are fixed, and that we cannot vary $\Omega(t)$ at these points: $\Omega(0)=\Omega(t)=0$. Obviously this integral, which represents the density of trajectories that has the proper features (prescribed initial and final conditions and photon speed equal to 1), is not trivial. However, for the sake of simplicity, we can approximate this density by considering that trajectories that have correct boundary conditions and average photon speeds equal to unity:

$$J(\dot{\mathbf{r}}(t))=Q\delta\left[\int_0^T(\mathbf{r}^2-1)dt\right]=\frac{Q}{2\pi}\int_{-\infty}^{+\infty}\exp\left[i\omega\int_0^T dt(\dot{\mathbf{r}}_i^2-1)\right]d\omega\ , \tag{A3}$$

where constant Q can be determined from normalization of the probability.

APPENDIX B: CLASSICAL PATH

The real part of effective Lagrangian,

$$L_{\text{eff}}=\frac{1}{2\mu_S(1-g)}[\ddot{\mathbf{r}}(t)]^2\ , \tag{B1}$$

can be minimized using Euler's equation

$$\frac{d^2}{dt^2}\left[\frac{\partial L_{\text{eff}}}{\partial\ddot{\mathbf{r}}}\right]=0 \tag{B2}$$

to give the solution of the form

$$\mathbf{r}_{\text{cl}}(t)=\mathbf{a}t^3+\mathbf{b}t^2+\mathbf{c}t+\mathbf{d}\ , \tag{B3}$$

which we will call a classical path [2,4], where **a**, **b**, **c**, and **d** are constant vectors that can be found from initial and final conditions on the trajectory: $\mathbf{r}(0)=0$, $(0)=\mathbf{v}_0$, $\mathbf{r}(T)=\mathbf{r}$, $(T)=\mathbf{v}_T$. It gives the following equation for the classical path:

$$\mathbf{r}_{\text{cl}}(t)=\frac{(\mathbf{v}_T+\mathbf{v}_0)T-2\mathbf{R}}{T^3}t^3+\frac{3\mathbf{R}-(\mathbf{v}_T+2\mathbf{v}_0)T}{T^2}t^2+\mathbf{v}_0t\ . \tag{B4}$$

APPENDIX C: APPROXIMATE FORM OF THE INTEGRAL FOR THE SMALL ANGLE SCATTERING REGIME

We can approximate $\mathbf{q}(t)$ in the form of series by sine's square, that give us the right initial and final conditions for the function and its first derivatives:

$$\mathbf{q}(t)=\sum_{n=1}^{N/2}\mathbf{a}_n\sin^2\frac{n\pi t}{T}\ . \tag{C1}$$

Obviously, this representation of $\mathbf{q}(t)$ is an approximation because the functions we choose do not form a full space. However, we believe they can give a decent presentation for variation of the trajectory. The integral we have to estimate is

$$I=\int_0^T\left[\frac{1}{2\mu_S(1-g)}\ddot{\mathbf{q}}^2-i\omega(2\dot{\mathbf{r}}_{\text{cl}}\dot{\mathbf{q}}+\dot{\mathbf{q}}^2)\right]dt\ , \tag{C2}$$

By substituting Eq. (C1) into Eq. (C2), we have

$$I=\int_0^T\left[\left\{\frac{1}{2\mu_S(1-g)}\sum_{n=1}^{N/2}\sum_{k=1}^{N/2}\mathbf{a}_n\mathbf{a}_k\frac{4n^2k^2\pi^4}{T^4}\cos\frac{2n\pi t}{T}\cos\frac{2k\pi t}{T}\right\}-i\omega\left\{2\dot{\mathbf{r}}_{\text{cl}}(t)\sum_{n=1}^{N/2}\mathbf{a}_n\frac{n\pi t}{T}\sin\frac{2n\pi t}{T}+\sum_{n=1}^{N/2}\sum_{k=1}^{N/2}\mathbf{a}_n\mathbf{a}_n\frac{nk\pi^2}{T^2}\sin\frac{2n\pi t}{T}\sin\frac{2k\pi t}{T}\right\}\right]dt\ . \tag{C3}$$

In the first approximation, the second term in Eq. (C3) can be neglected. This gives

$$I\cong\sum_{n=1}^{N/2}\left[\frac{2n^4\pi^4}{\mu_S(1-g)T^3}-i\omega\frac{n^2\pi^2}{2T}\right]\mathbf{a}_n^2\ . \tag{C4}$$

We can then rewrite Eq. (19) in the form

$$P(\mathbf{r}_A,\mathbf{r}_B,T)\cong F(T)\exp\left[-\int_0^T\frac{1}{2\mu_S(1-g)}\ddot{\mathbf{r}}_{\text{cl}}^2dt\right]\times\int_{-\infty}^{+\infty}d\omega\exp\left[i\omega\int_0^T(\dot{\mathbf{r}}_{\text{cl}}^2-1)dt\right]\prod_{n=1}^{N/2}\left[\frac{4n^2\pi^2}{\mu_S(1-g)T^2}-i\omega\right]^{-3/2}\ . \tag{C5}$$

The last integral is approximately equal to [9]:

$$P(\mathbf{r}_A,\mathbf{r}_B,T)\cong F(T)\exp\left[-\int_0^T\frac{1}{2\mu_S(1-g)}\ddot{\mathbf{r}}_{\text{cl}}^2dt\right]\exp\left\{-\frac{3\mu_S(1-g)T^2}{4}\left[\int_0^T(\dot{\mathbf{r}}_{\text{cl}}^2-1)dt\right]^{-1}\right\}\ . \tag{C6}$$

[1] *Advances in Photon Migration Imaging and Optical Tomography,* edited by R. R. Alfano (Optical Society of America, Washington, D.C., 1994), and references therein.
[2] L. T. Perelman, J. Wu, I. Itzkan, and M. S. Feld, Phys. Rev. Lett. **71**, 1341 (1994).
[3] J. Tessendorf, Phys. Rev. A **35**, 872 (1988).
[4] L. T. Perelman, J. Wu, I. Itzkan, Y. Wang, R. R. Dasari, and M. S. Feld, in *Advances in Photon Migration Imaging and Optical Tomography,* edited by R. R. Alfano (Optical Society of America, Washington, D.C., 1994).
[5] A. Ishimaru, *Wave Propagation and Scattering in Random Media* (Academic, Orlando, 1978).
[6] R. P. Feynman and A. R. Hibbs, *Quantum Mechanics and Path Integrals* (McGraw-Hill, New York, 1965).
[7] I. S. Gradstein and I. M. Ryzhik, *Tables of Integrals, Series, and Products* (Academic, London, 1980).
[8] H. J. van Staveren, C. J. M. Moes, J. van Marle, S. A. Prahl, and M. J. C. van Gemert, Appl. Opt. **30**, 4507 (1991).
[9] A. P. Prudnikov, Yu. A. Brychkov, O. I. Marichev, *Integrals and Series* (Gordon and Breach, New York, 1986).